

Repeater-Assisted Massive MIMO Downlink Performance with Calibration Errors

Kohei Ueda*, Anubhab Chowdhury†, Koji Ishibashi*, and Erik G. Larsson†

*Advanced Wireless & Communication Research Center (AWCC), The University of Electro-Communications, 1-5-1 Chofugaoka, Chofu, Tokyo 182-8585, Japan

†Department of Electrical Engineering (ISY), Linköping University, 58183 Linköping, Sweden
Emails: *k.ueda@awcc.uec.ac.jp, †anuch87@liu.se, *koji@ieee.org, and †erik.g.larsson@liu.se

Abstract—Reciprocity-based downlink beamforming is imperative for a scalable time-division duplex massive multiple-input multiple-output (MIMO) deployment. Specifically, for a dual-antenna repeater-assisted massive MIMO system, a mismatch between forward and reverse path gains at the repeater can exacerbate the overall calibration error between the user equipments (UEs) and the base station (BS), which potentially also contains calibration errors of their individual radio-frequency chains. This paper models the effects of such calibration errors, underpins the relations between the uplink and downlink channels for repeater-assisted systems with calibration errors clubbed with the over-the-air channel estimation errors, and derives analytical expressions of the downlink spectral efficiency. The presented results can then be simplified to several special cases, underscoring situations wherein such errors can become pronounced.

Index Terms—Repeater, Massive MIMO, Reciprocity calibration, TDD.

I. INTRODUCTION

Repeaters are full-duplex devices that instantaneously receive and retransmit signals within a given band, in a way transparent to the network, acting as ordinary channel scatterers but with amplification. Repeaters can be deployed on a large scale to mitigate coverage holes for cellular multiple-input multiple-output (MIMO) wireless systems [1]–[6]. In [1], it is demonstrated that repeaters procure spectral efficiency (SE) similar to distributed MIMO while obviating the front-haul signaling overhead required by the latter. Specifically, dual-antenna repeater technology has been included in the 5G NR standards since 3rd Generation Partnership Project (3GPP) Release 18 [7], named as network-controlled repeater (NCR).

For dual-antenna repeaters to appear transparent to the base station (BS) and the user equipments (UEs), they need to be reciprocity calibrated, i.e., the forward and the reverse path gains should be equal. In this regard, [8] developed a non-linear least-squares framework to estimate the ratio of the forward to reverse path gains of a repeater, following which a compensation for the mismatch in the uplink/downlink antenna path gains can be executed. Further, the propounded strategy in [8] also extends to multiple repeaters.

Nonetheless, the over-the-air calibration techniques heavily rely on the channel estimates, which in turn are prone to

errors. When reciprocity-based beamforming is applied in the downlink massive MIMO system, the calibration error degrades the beamforming gain, and consequently the overall downlink SE [9]–[12]. With regard to repeater-assisted systems, [13] investigated the effects of mismatched forward and reverse link gains at the repeaters on the downlink signal-to-interference-plus-noise ratio (SINR). However, the results therein ignore the direct link channel between the BS and the UEs, and are restricted to errors only in the repeaters' calibration coefficients, and highly depend on large-dimensional approximations.

Our proposed framework considers both channel estimation and calibration errors in all transceiver chains between the BS and the UEs, i.e., the direct link channels and the channels via the repeater. Thus, the model presented in [13] can be subsumed as a special case of our analysis. We obtain expressions for the downlink SE via achievable rate analysis for finite numbers of antennas. These results quantify the composite effects of calibration errors at the BS, the UEs, and the repeaters.

Notation: The identity matrix of size N and the all-zero column vector of size N are denoted by \mathbf{I}_N and $\mathbf{0}_N$, respectively. A circularly symmetric complex Gaussian (CSCG) with mean vector $\boldsymbol{\mu}$ and covariance matrix $\boldsymbol{\Sigma}$ is denoted by $\mathcal{CN}(\boldsymbol{\mu}, \boldsymbol{\Sigma})$. The operators $(\cdot)^*$, $(\cdot)^T$, $(\cdot)^H$, and \odot denote conjugate, transpose, Hermitian transpose, and element-wise product, respectively. The operators $\mathbb{E}[\cdot]$, $\text{Var}(\cdot)$, $\text{Tr}\{\cdot\}$ and $\|\cdot\|$ are expectation, variance, trace of a matrix, and ℓ_2 -norm, respectively. For a diagonal matrix \mathbf{D} , $|\mathbf{D}|$ implies element-wise absolute values.

II. SYSTEM MODEL

We consider a dual-antenna repeater-assisted massive MIMO (RA-MIMO) system where K UEs are being served by a massive MIMO BS [8], operating in time-division duplex (TDD). The BS is equipped with N antennas, and UEs are all single-antenna. The diagonal matrices \mathbf{T}_B and $\mathbf{R}_B \in \mathbb{C}^{N \times N}$ consist of the transmit and receive reciprocity coefficients, with the n -th diagonal element being $\{t_{B,n}\}$ and $\{r_{B,n}\}$, corresponding to the n -th BS antenna, respectively. Similarly, the corresponding coefficients for the k -th UE are denoted by $\{t_{U,k}\}$ and $\{r_{U,k}\}$ [14]. Let α_u and α_d be the forward and reverse link complex-valued gains of the repeater [8]. Next,

This work was supported in part by the KAW foundation, ELLIIT, the Swedish Research Council (VR), JST CRONOS, Japan Grant Number JPMJCS24N1, and JST BOOST, Japan Grant Number JPMJBS2415.

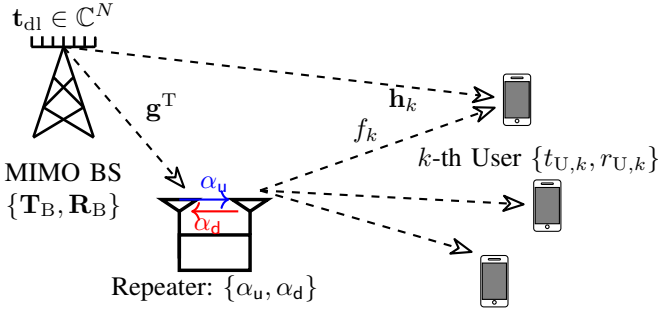


Fig. 1. Repeater-assisted communication. Dashed lines (---) indicate over-the-air channels that are reciprocal. Solid lines (—) in blue and red along the repeater show the forward and reverse path gains of the transceiver chains.

the over-the-air (uplink) channels from the k -th UE to the BS, the repeater to the BS, and the repeater to the k -th UE are denoted by $\mathbf{h}_k \in \mathbb{C}^{N \times 1}$, $\mathbf{g} \in \mathbb{C}^{N \times 1}$, and $f_k \in \mathbb{C}$, respectively. These over-the-air channels are reciprocal. Thus, the equivalent uplink channel from the k -th UE to the BS can be written as:

$$\mathbf{h}_{\text{ul},k} = \bar{\mathbf{h}}_{\text{ul},k} + \bar{\mathbf{g}}_{\text{ul},k}, \quad (1)$$

where the direct link equivalent channel $\bar{\mathbf{h}}_{\text{ul},k}$ and the over-the-air uplink channel \mathbf{h}_k are related as

$$\bar{\mathbf{h}}_{\text{ul},k} = t_{U,k} \mathbf{R}_B \mathbf{h}_k. \quad (2)$$

We note that the over-the-air channel \mathbf{h}_k is measured with the repeater being turned off; however, it can contain (reciprocal) passive scattering effects of the repeater. The equivalent uplink channel from the UE to the BS via the repeater $\bar{\mathbf{g}}_{\text{ul},k}$ is

$$\bar{\mathbf{g}}_{\text{ul},k} = \alpha_u t_{U,k} \mathbf{R}_B \{ \mathbf{g} f_k \}. \quad (3)$$

Next, the equivalent downlink channel for the k -th UE can be expressed as

$$\begin{aligned} \mathbf{h}_{\text{dl},k}^T &= r_{U,k} \mathbf{h}_k^T \mathbf{T}_B + \alpha_d r_{U,k} \{ f_k \mathbf{g}^T \} \mathbf{T}_B \\ &= \frac{r_{U,k}}{t_{U,k}} \left(\bar{\mathbf{h}}_{\text{ul},k}^T + \frac{\alpha_d}{\alpha_u} \bar{\mathbf{g}}_{\text{ul},k}^T \right) \mathbf{R}_B^{-1} \mathbf{T}_B, \end{aligned} \quad (4)$$

where we used the fact that \mathbf{T}_B and \mathbf{R}_B are diagonal. To capture the mismatches in the calibration coefficients, we define $e_{U,k} = \frac{r_{U,k}}{t_{U,k}}$, $\mathbf{E}_B = \mathbf{R}_B^{-1} \mathbf{T}_B$ with the n -th diagonal element being $e_{B,n}$, and $e_R = \frac{\alpha_d}{\alpha_u}$. Thus, after taking transpose of (4), we get

$$\mathbf{h}_{\text{dl},k} = e_{U,k} \mathbf{E}_B (\bar{\mathbf{h}}_{\text{ul},k} + e_R \bar{\mathbf{g}}_{\text{ul},k}), \quad (5)$$

which establishes the relation between the equivalent uplink and downlink channels for repeater-assisted systems with reciprocity imperfections.

1) *Modeling Calibration Errors:* In practice, $e_{U,k}$, \mathbf{E}_B , and e_R need to be calibrated and compensated [8], so that the repeater acts transparent to the UEs and the BS, and BS can use reciprocity-based beamforming. However, the calibration errors cannot be avoided due to the noisy measurements during the over-the-air calibration process. We capture such errors in calibration as [14]: $e_{U,k} = \hat{e}_{U,k} + \tilde{e}_{U,k}$, $\mathbf{E}_B =$

$\hat{\mathbf{E}}_B + \tilde{\mathbf{E}}_B$, and $e_R = \hat{e}_R + \tilde{e}_R$, where $\hat{e}_{U,k}$, $\hat{\mathbf{E}}_B$, and \hat{e}_R are the estimated ‘‘mismatched’’ coefficients and assumed to be *known* [10]. The errors in the calibration are captured by $\tilde{e}_{U,k}$, $\tilde{\mathbf{E}}_B$, and \tilde{e}_R , which are zero mean random variables with variances/covariance being $\sigma_{U,k}^2$, $\sigma_B^2 \mathbf{I}_N$, and σ_R^2 , respectively. Also, calibration errors across UEs are independent.

2) *Impact on Uplink Channel Estimation:* As a necessary first step to understand the effects of calibration error on system performance, we consider a noiseless repeater and abstract the channel estimation procedure. We consider $\bar{\mathbf{h}}_{\text{ul},k} = \hat{\mathbf{h}}_{\text{ul},k} + \tilde{\mathbf{h}}_{\text{ul},k}$ and $\bar{\mathbf{g}}_{\text{ul},k} = \hat{\mathbf{g}}_{\text{ul},k} + \tilde{\mathbf{g}}_{\text{ul},k}$, where $\hat{\mathbf{x}}$ denotes the estimate of a variable \mathbf{x} , and $\tilde{\mathbf{x}}$ the estimation error. Then, the equivalent downlink channel in (6) becomes

$$\begin{aligned} \mathbf{h}_{\text{dl},k} &= (\hat{e}_{U,k} + \tilde{e}_{U,k}) (\hat{\mathbf{E}}_B + \tilde{\mathbf{E}}_B) \left(\left\{ \hat{\mathbf{h}}_{\text{ul},k} + \tilde{\mathbf{h}}_{\text{ul},k} \right\} \right. \\ &\quad \left. + (\hat{e}_R + \tilde{e}_R) \left\{ \hat{\mathbf{g}}_{\text{ul},k} + \tilde{\mathbf{g}}_{\text{ul},k} \right\} \right) \triangleq \hat{\mathbf{h}}_{\text{dl},k} + \tilde{\mathbf{h}}_{\text{dl},k}, \end{aligned} \quad (6)$$

where, with a little algebra, the estimated equivalent downlink channel and the error vector can respectively be expressed as:

$$\hat{\mathbf{h}}_{\text{dl},k} = \hat{e}_{U,k} \hat{\mathbf{E}}_B (\hat{\mathbf{h}}_{\text{ul},k} + \hat{e}_R \hat{\mathbf{g}}_{\text{ul},k}) = \hat{e}_{U,k} \hat{\mathbf{E}}_B \hat{\mathbf{h}}_{\text{ul},k} \quad (7a)$$

$$\tilde{\mathbf{h}}_{\text{dl},k} = \tilde{e}_{U,k} \hat{\mathbf{E}}_B \hat{\mathbf{h}}_{\text{ul},k} + e_{U,k} (\tilde{\mathbf{E}}_B \hat{\mathbf{h}}_{\text{ul},k} + \hat{\mathbf{E}}_B \tilde{\mathbf{h}}_{\text{ul},k} + \tilde{\mathbf{E}}_B \hat{\mathbf{h}}_{\text{ul},k}), \quad (7b)$$

where $\hat{\mathbf{h}}_{\text{ul},k} \triangleq \hat{\mathbf{h}}_{\text{ul},k} + \hat{e}_R \hat{\mathbf{g}}_{\text{ul},k}$ and $\tilde{\mathbf{h}}_{\text{ul},k} \triangleq \tilde{\mathbf{h}}_{\text{ul},k} + e_R \tilde{\mathbf{g}}_{\text{ul},k} + \tilde{e}_R \hat{\mathbf{g}}_{\text{ul},k}$. It is clear from (7b) that $\tilde{\mathbf{h}}_{\text{dl},k}$ is also affected by the uplink estimated channels as well as the errors due to the multiplicative nature of the calibration coefficients. Thus, a calibration error can potentially increase the variance of the error in the effective estimated downlink channel, thereby degrading the SE, which is discussed next.

III. EFFECTS OF CALIBRATION ERROR ON DOWNLINK SE

In this section, we analyze the ergodic capacity with respect to channels, estimation errors of the channel and calibration coefficient, and noise, conditioned on a given estimate of the calibration coefficients. Using $\hat{\mathbf{h}}_{\text{dl},k}$ in (7a), the signal received at the k -th UE can be expressed as:

$$\hat{s}_k = \sqrt{\rho \kappa_k} \mathbf{h}_{\text{dl},k}^T \hat{\mathbf{h}}_{\text{dl},k}^* s_k + \sum_{n \neq k} \sqrt{\rho \kappa_n} \mathbf{h}_{\text{dl},k}^T \hat{\mathbf{h}}_{\text{dl},n}^* s_n + w_k, \quad (8)$$

where ρ is the total downlink transmit power, $\kappa_k = \frac{\eta_k}{\text{Tr}\{\mathbb{E}[\mathbf{h}_{\text{dl},k} \mathbf{h}_{\text{dl},k}^H]\}}$, $\eta_k \in [0, 1]$ is the power allocation variable including channel gain normalization of the k -th UE, and s_k is the unit-energy zero-mean data symbol intended for the k -th UE. $w_k \sim \mathcal{CN}(0, \sigma_{\text{UE}}^2)$ is the additive white Gaussian noise (AWGN) at the k -th UE. Further, we can rewrite \hat{s}_k , following the principle of use-and-then-forget bound [15], as

$$\hat{s}_k = \sqrt{\rho \kappa_k} \mathbb{E} \left[\hat{\mathbf{h}}_{\text{dl},k}^T \hat{\mathbf{h}}_{\text{dl},k}^* \right] s_k + z_k, \quad (9)$$

where the expectation is taken with respect to the randomness in the channels and the calibration errors. Then, the effective interference-plus-AWGN z_k constitutes

$$z_k = \sqrt{\rho\kappa_k} \left(\hat{\mathbf{h}}_{\text{dl},k}^T \hat{\mathbf{h}}_{\text{dl},k}^* - \mathbb{E} \left[\hat{\mathbf{h}}_{\text{dl},k}^T \hat{\mathbf{h}}_{\text{dl},k}^* \right] \right) s_k \quad (10)$$

$$+ \sqrt{\rho\kappa_k} \tilde{\mathbf{h}}_{\text{dl},k}^T \hat{\mathbf{h}}_{\text{dl},k}^* s_k + \sum_{n \neq k} \sqrt{\rho\kappa_n} \hat{\mathbf{h}}_{\text{dl},k}^T \hat{\mathbf{h}}_{\text{dl},n}^* s_n + w_k.$$

Proposition 1. *If the estimated uplink channels $\hat{\mathbf{h}}_{\text{ul},k}$ and $\hat{\mathbf{g}}_{\text{ul},k}$ are uncorrelated with the errors $\tilde{\mathbf{h}}_{\text{ul},k}$ and $\tilde{\mathbf{g}}_{\text{ul},k}$, it can be shown that $\hat{\mathbf{h}}_{\text{dl},k}$ is uncorrelated with $\tilde{\mathbf{h}}_{\text{dl},k}$; and consequently, z_k is uncorrelated with $\mathbb{E}[\hat{\mathbf{h}}_{\text{dl},k}^T \hat{\mathbf{h}}_{\text{dl},k}^*] s_k$.*

Next, thanks to Theorem 1, a use-and-then-forget type [15] lower bound on the downlink SE of the k -th UE can be evaluated as $R_k = \log(1 + \text{SINR}_k)$, where the downlink SINR is computed as $\text{SINR}_k \triangleq |\sqrt{\rho\kappa_k} \mathbb{E}[\hat{\mathbf{h}}_{\text{dl},k}^T \hat{\mathbf{h}}_{\text{dl},k}^*]|^2 / \mathbb{E}[|z_k|^2]$. This, we can further break down as follows:

$$\text{SINR}_k = \frac{G_k}{\text{BI}_k + \text{CI}_k + \text{MI}_k + \sigma_{\text{UE}}^2}, \quad (11)$$

where the terms are defined as

$$G_k \triangleq \rho\kappa_k \left| \mathbb{E} \left[\hat{\mathbf{h}}_{\text{dl},k}^T \hat{\mathbf{h}}_{\text{dl},k}^* \right] \right|^2, \quad (12a)$$

$$\text{BI}_k \triangleq \rho\kappa_k \text{Var} \left(\hat{\mathbf{h}}_{\text{dl},k}^T \hat{\mathbf{h}}_{\text{dl},k}^* \right), \quad (12b)$$

$$\text{CI}_k \triangleq \rho\kappa_k \mathbb{E} \left[\left| \tilde{\mathbf{h}}_{\text{dl},k}^T \hat{\mathbf{h}}_{\text{dl},k}^* \right|^2 \right], \quad (12c)$$

$$\text{MI}_k \triangleq \sum_{n \neq k} \rho\kappa_n \mathbb{E} \left[\left| \hat{\mathbf{h}}_{\text{dl},k}^T \hat{\mathbf{h}}_{\text{dl},n}^* \right|^2 \right]; \quad (12d)$$

and they are respectively the array gain, the variance of the beamforming uncertainty, self-interference due to calibration imperfections, and multi-UE interference, all at the k -th UE. We note that the SINR in (11) can be evaluated for any channel model. However, to obtain an intuitive understanding of the effects of imperfect calibration on the downlink SINR, a mathematically tractable closed-form expression of (11) is required. This further depends on the underlying distributions of the channels. Due to the multiplicative nature of the calibration coefficients and the composite channels, we consider the following simplifications.

First of all, we assume perfect channel state information (CSI) for the repeater to the BS (i.e., \mathbf{g}).¹ Then, to capture the effects of uplink channel estimation errors, we consider $\hat{\mathbf{h}}_{\text{ul},k} \sim \mathcal{CN}(\mathbf{0}_N, \mathbf{K}_{\hat{\mathbf{h}}_k})$ and $\tilde{\mathbf{h}}_{\text{ul},k} \sim \mathcal{CN}(\mathbf{0}_N, \mathbf{\Sigma}_{\tilde{\mathbf{h}}_k} - \mathbf{K}_{\hat{\mathbf{h}}_k})$, where $\tilde{\mathbf{h}}_{\text{ul},k} \sim \mathcal{CN}(\mathbf{0}_N, \mathbf{\Sigma}_{\tilde{\mathbf{h}}_k})$ and $\mathbf{\Sigma}_{\tilde{\mathbf{h}}_k} = \beta_{h_k} |t_{U,k}|^2 \mathbf{R}_B \mathbf{R}_B^H$. Similarly, if we assume $\tilde{\mathbf{g}}_{\text{ul},k} \sim \mathcal{CN}(\mathbf{0}_N, \mathbf{\Sigma}_{\tilde{\mathbf{g}}_k})$, we can write $\hat{\mathbf{g}}_{\text{ul},k} \sim \mathcal{CN}(\mathbf{0}_N, \mathbf{K}_{\hat{\mathbf{g}}_k})$ and $\tilde{\mathbf{g}}_{\text{ul},k} \sim \mathcal{CN}(\mathbf{0}_N, \mathbf{\Sigma}_{\tilde{\mathbf{g}}_k} - \mathbf{K}_{\hat{\mathbf{g}}_k})$, where $\mathbf{\Sigma}_{\tilde{\mathbf{g}}_k} = \beta_{f_k} |\alpha_u|^2 |t_{U,k}|^2 \mathbf{R}_B \mathbf{g} \mathbf{g}^H \mathbf{R}_B^H$. Here, assuming the orthogonal pilot and minimum mean-squared error (MMSE)

¹This assumption, although optimistic, is fairly reasonable in practical scenarios as typically the BS and the repeater would be deployed at elevated locations (e.g., rooftops) and within line-of-sight (LoS) of one another.

estimator for the channel estimation, we can define the covariance matrices corresponding to the above variables as follows:

$$\mathbf{K}_{\hat{\mathbf{h}}_k} = \rho_{\text{UL}} \mathbf{\Sigma}_{\hat{\mathbf{h}}_k} \left(\rho_{\text{UL}} \mathbf{\Sigma}_{\hat{\mathbf{h}}_k} + \sigma_{\text{BS}}^2 \mathbf{I}_N \right)^{-1} \mathbf{\Sigma}_{\hat{\mathbf{h}}_k} \quad (13a)$$

$$\mathbf{K}_{\hat{\mathbf{g}}_k} = \rho_{\text{UL}} \mathbf{\Sigma}_{\hat{\mathbf{g}}_k} \left(\rho_{\text{UL}} \mathbf{\Sigma}_{\hat{\mathbf{g}}_k} + \sigma_{\text{BS}}^2 \mathbf{I}_N \right)^{-1} \mathbf{\Sigma}_{\hat{\mathbf{g}}_k}, \quad (13b)$$

where ρ_{UL} denotes the uplink transmit power. Further, we consider that orthogonality between the estimated channels and the error vectors (which holds for MMSE estimators) and the independence between the estimated direct-link channel and the channel via the repeater. Then $\hat{\mathbf{h}}_{\text{ul},k}$ is zero-mean CSCG random vector with covariance being $\mathbf{\Sigma}_{\hat{\mathbf{h}}_{\text{ul},k}} = \mathbf{K}_{\hat{\mathbf{h}}_k} + |\hat{e}_R|^2 \mathbf{K}_{\hat{\mathbf{g}}_k}$. However, we acknowledge that $\hat{\mathbf{h}}_{\text{ul},k}$ is not Gaussian, since it contains products of random variables such as $\tilde{e}_U \mathbf{E}_B \tilde{\mathbf{h}}_{\text{ul},k}$. The computation joint distribution of these variables is not mathematically amenable and beyond the scope of this paper. Thus, we approximate $\hat{\mathbf{h}}_{\text{ul},k}$ by a CSCG random vector with the covariance being $\mathbf{\Sigma}_{\hat{\mathbf{h}}_{\text{ul},k}} \triangleq (\mathbf{\Sigma}_{\tilde{\mathbf{h}}_k} - \mathbf{K}_{\hat{\mathbf{h}}_k}) + |\hat{e}_R|^2 (\mathbf{\Sigma}_{\tilde{\mathbf{g}}_k} - \mathbf{K}_{\hat{\mathbf{g}}_k}) + \sigma_{\text{R}}^2 \mathbf{\Sigma}_{\tilde{\mathbf{g}}_k}$. With these, we can now compute the SINR in closed form.

Theorem 2. *The downlink SINR of the k -th UE with imperfectly calibrated reciprocity coefficients can be written as*

$$\frac{\kappa_k |\hat{e}_{U,k}|^4 \left| \text{Tr} \left\{ \mathbf{\Sigma}_{\hat{\mathbf{h}}_{\text{ul},k}} | \hat{\mathbf{E}}_B \right\} \right|^2}{\sum_{n=1}^K \delta_{kn} \mu_{kn} + \sigma_{\text{B}}^2 \left(\delta_{kk} \dot{\xi}_{kk} + \sum_{n \neq k} \delta_{kn} \xi_{kn} \right) + \delta_{kk} \nu_{kk} + \frac{\sigma_{\text{UE}}^2}{\rho}}, \quad (14)$$

where the terms are defined as follows:

$$\delta_{kn} = \kappa_n |\hat{e}_{U,n}|^2 \left(|\hat{e}_{U,k}|^2 + \sigma_{U,k}^2 \right), \quad (15a)$$

$$\dot{\delta}_{kk} = \kappa_k |\hat{e}_{U,k}|^2 \sigma_{U,k}^2, \quad (15b)$$

$$\mu_{kn} = \text{Tr} \left\{ \left(\mathbf{\Sigma}_{\hat{\mathbf{h}}_{\text{ul},k}} + \mathbf{\Sigma}_{\tilde{\mathbf{h}}_{\text{ul},k}} \right) | \hat{\mathbf{E}}_B \right\}^2 \mathbf{\Sigma}_{\hat{\mathbf{h}}_{\text{ul},n}} | \hat{\mathbf{E}}_B \right\}^2, \quad (15c)$$

$$\xi_{kn} = \text{Tr} \left\{ \left(\hat{\mathbf{E}}_B^* \mathbf{\Sigma}_{\hat{\mathbf{h}}_{\text{ul},n}} \hat{\mathbf{E}}_B^T \right) \odot \left(\mathbf{\Sigma}_{\hat{\mathbf{h}}_{\text{ul},k}} + \mathbf{\Sigma}_{\tilde{\mathbf{h}}_{\text{ul},k}} \right)^T \right\}, \quad (15d)$$

$$\dot{\xi}_{kk} = \text{Tr} \left\{ \hat{\mathbf{E}}_B^* \mathbf{\Sigma}_{\hat{\mathbf{h}}_{\text{ul},k}} \odot \left(\hat{\mathbf{E}}_B^* \mathbf{\Sigma}_{\hat{\mathbf{h}}_{\text{ul},k}} \right)^H \right\} + \xi_{kk}, \quad (15e)$$

$$\nu_{kk} = \left| \text{Tr} \left\{ \mathbf{\Sigma}_{\hat{\mathbf{h}}_{\text{ul},k}} | \hat{\mathbf{E}}_B \right\} \right|^2. \quad (15f)$$

Proof. See Appendix A. ■

Observation 1. *The part of interference in the downlink SINR which arises only due to the effects of calibration imperfections can be shown to be equal to $\left\{ \sum_{n=1}^K \kappa_n |\hat{e}_{U,n}|^2 \sigma_{U,k}^2 \mu_{kn} + \sigma_{\text{B}}^2 (\delta_{kk} \dot{\xi}_{kk} + \sum_{n \neq k} \delta_{kn} \xi_{kn}) + \sigma_{\text{U},k}^2 \kappa_k |\hat{e}_{U,k}|^2 \nu_{kk} \right\}$, where the constituent terms explicitly depend on the error variances, $\{\sigma_{U,k}^2, \sigma_{\text{B}}^2\}$, in measuring the calibration coefficients at the BS and the UEs. This implies that the calibration errors at the BS and UEs are physically embedded in the transceiver RF chains and hence affect all effective channels. In contrast, the repeater calibration error variance σ_{R}^2 affects only the covariance $\mathbf{\Sigma}_{\hat{\mathbf{h}}_{\text{ul},k}}$ in ξ_{kn} , since it impacts only the channel components that traverse the repeater path.*

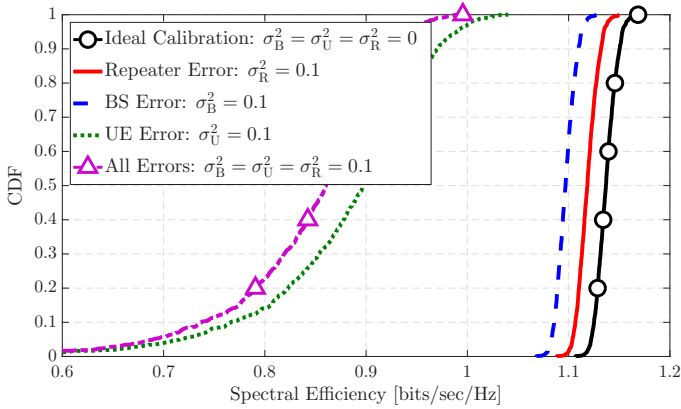


Fig. 2. CDFs of SE with different calibration error variance. In the legend, whenever a variance (e.g., $\sigma_R^2 = 0.1$) is specified, the other variances are set to zero.

1) Special case: No calibration error at the BS and UEs:

For this, $e_{U,k} = \hat{e}_{U,k} = 1, \forall k$, and $\mathbf{E}_B = \hat{\mathbf{E}}_B = \mathbf{I}_N$. This case subsumes the results presented in [13].

While for ease of exposure, herein we consider a single repeater, the preceding analyses can be generalized to multiple repeaters. Conceptually, this extension is straightforward, but it entails substantial additional bookkeeping. For example, under independence assumptions across the repeater-related channels, the covariance expressions follow in a straightforward manner.

IV. NUMERICAL RESULTS AND DISCUSSIONS

In this section, we provide the numerical results of the SE analyzed based on the proposed framework. We consider a circular cell with a radius of 650 [m], where the BS, equipped with $N = 64$ antennas, is located at the center. The repeater is located 200 [m] away from the BS along the 0° direction, and $K = 10$ UEs are randomly distributed within the cell.

We employ the same channel model as in [5] while assuming that a LoS BS–repeater link always exists by carefully deploying the repeater. Carrier frequency, bandwidth, and noise density are set to $f_c = 6$ [GHz], $B = 20$ [MHz], and -174 [dBm/Hz], respectively [5]. The transmit powers of the BS, UE (for uplink channel estimation), and repeater are set to $\rho = 33$ [dBm], $\rho_{UL} = 23$ [dBm], and $\rho_R = 23$ [dBm], respectively. The repeater amplification gain is given by $\alpha = \min(\sqrt{\rho_R/(\rho\beta_g)}, A_{\max})$, where β_g and $A_{\max} = 90$ [dB] denote path-loss of BS–repeater channel and maximum amplification gain, respectively. In the simulation, following [11], we model the calibration error as $e_Z = 1 + \mathcal{CN}(0, \sigma_Z^2)$, $Z \in \{B, U, R\}$, and 100 such random calibration error realizations are considered for cumulative distribution function (CDF) computations. Then, we define the “ideal calibration” case as $\sigma_R^2 = \sigma_B^2 = \sigma_U^2 = 0$. For simplicity, we further assume $\alpha_u = \min(\sqrt{\rho_R/(\rho\beta_g)}, A_{\max})$, $t_{U,k} = 1, \forall k$, and $\mathbf{R}_B = \mathbf{I}_N$.

Fig. 2 and Fig. 3 illustrate the CDF of the SE obtained from (14) and the 90th-percentile SE performance as a function of the error variance, respectively. From Fig. 2, it can be

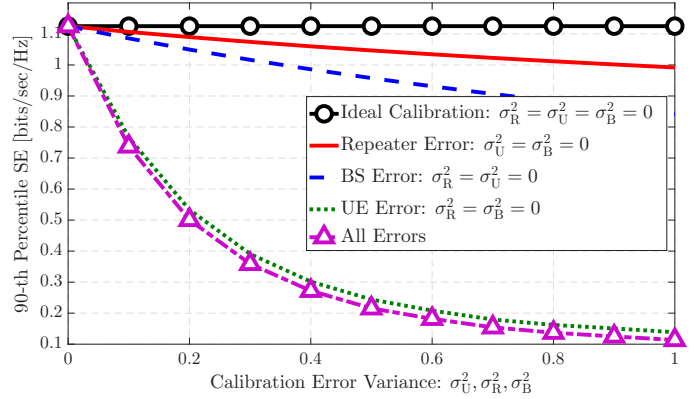


Fig. 3. 90-th percentile SE as a function of calibration error variance.

observed that the performance loss caused by the repeater calibration error is smaller than that caused by the other errors. This is because, as noted in Observation 1, the repeater calibration error affects only $\Sigma_{\hat{\mathbf{h}}_{ul,k}}$ linearly, whereas the UE error impacts all interference terms. When the error variance is small, the performance loss due to the BS error is close to that of the repeater error. However, as shown in both figures, the performance gap between the BS error and the repeater error grows with the error variance, even though the losses in both cases increase approximately linearly. In contrast to σ_R^2 , which increases the interference power linearly with respect to $\Sigma_{\hat{\mathbf{h}}_{ul,k}}$, σ_B^2 increases it linearly with respect to $(\delta_{kk}\xi_{kk} + \sum_{n \neq k} \delta_{kn}\xi_{kn})$, which includes $\Sigma_{\hat{\mathbf{h}}_{ul,k}}$ (see (15d)). As a result, the performance gap between the BS error and the repeater error widens as the calibration error variance increases.

V. CONCLUSION

This paper has proposed an SE evaluation framework that accounts for imperfect channel estimation and calibration. Compared with previous work that considered only repeater calibration errors [13], our framework extends the analysis to include BS and UE calibration mismatches. The numerical results demonstrated that the impact of repeater calibration errors is smaller than that of BS and UE calibration errors in the considered single-repeater system with Gaussian error modeling. Nonetheless, this indicates that repeater-assisted MIMO systems exhibit a certain level of robustness against repeater calibration errors. Thus, the system can operate with only minimal additional overhead for repeater calibration. However, quantifying the overhead per coherence block, including channel estimation and calibration overhead, remains to be addressed.

APPENDIX

A. Derivation of SINR_k for Theorem 2.

To compute the array gain, we evaluate the following.

$$\mathbb{E} \left[\hat{\mathbf{h}}_{dl,k}^T \hat{\mathbf{h}}_{dl,k}^* \right] = |\hat{e}_{U,k}|^2 \text{Tr} \left\{ \Sigma_{\hat{\mathbf{h}}_{ul,k}} \left| \hat{\mathbf{E}}_B \right|^2 \right\}, \quad (16)$$

which follows using Result 1. Next, we evaluate the variance term involved in BI_k . Using Result 1, we obtain

$$\begin{aligned} \mathbb{E} \left[|\hat{\mathbf{h}}_{\text{dl},k}^{\text{T}} \hat{\mathbf{h}}_{\text{dl},k}^*|^2 \right] &= |\hat{e}_{\text{U},k}|^4 \mathbb{E} \left[|\hat{\mathbf{h}}_{\text{ul},k}^{\text{T}} \hat{\mathbf{E}}_{\text{B}}|^2 |\hat{\mathbf{h}}_{\text{ul},k}^*|^2 \right] \\ &= |\hat{e}_{\text{U},k}|^4 \left(\left| \text{Tr} \left\{ \Sigma_{\hat{\mathbf{h}}_{\text{ul},k}} |\hat{\mathbf{E}}_{\text{B}}|^2 \right\} \right|^2 + \text{Tr} \left\{ \left(\Sigma_{\hat{\mathbf{h}}_{\text{ul},k}} |\hat{\mathbf{E}}_{\text{B}}|^2 \right)^2 \right\} \right). \end{aligned} \quad (17)$$

Based on this and (16), we get the final expression for BI_k as

$$\text{BI}_k = \rho \kappa_k |\hat{e}_{\text{U},k}|^4 \text{Tr} \left\{ \left(\Sigma_{\hat{\mathbf{h}}_{\text{ul},k}} |\hat{\mathbf{E}}_{\text{B}}|^2 \right)^2 \right\}. \quad (18)$$

Substituting $\tilde{\mathbf{h}}_{\text{dl},k}$ from (7b) and due to the mutual uncorrelatedness of the involved terms, the expectation in CI_k becomes

$$\begin{aligned} \mathbb{E} \left[|\tilde{\mathbf{h}}_{\text{dl},k}^{\text{T}} \hat{\mathbf{h}}_{\text{dl},k}^*|^2 \right] &= \mathbb{E} \left[\left| \tilde{e}_{\text{U},k} \hat{e}_{\text{U},k}^* \hat{\mathbf{h}}_{\text{ul},k}^{\text{T}} \hat{\mathbf{E}}_{\text{B}}^{\text{T}} \hat{\mathbf{E}}_{\text{B}}^* \hat{\mathbf{h}}_{\text{ul},k}^* \right|^2 \right] \\ &\quad + \mathbb{E} \left[\left| e_{\text{U},k} \hat{e}_{\text{U},k}^* \hat{\mathbf{h}}_{\text{ul},k}^{\text{T}} \tilde{\mathbf{E}}_{\text{B}}^{\text{T}} \tilde{\mathbf{E}}_{\text{B}}^* \hat{\mathbf{h}}_{\text{ul},k}^* \right|^2 \right] \\ &\quad + \mathbb{E} \left[\left| e_{\text{U},k} \hat{e}_{\text{U},k}^* \tilde{\mathbf{h}}_{\text{ul},k}^{\text{T}} \hat{\mathbf{E}}_{\text{B}}^{\text{T}} \hat{\mathbf{E}}_{\text{B}}^* \hat{\mathbf{h}}_{\text{ul},k}^* \right|^2 \right] \\ &\quad + \mathbb{E} \left[\left| e_{\text{U},k} \hat{e}_{\text{U},k}^* \tilde{\mathbf{h}}_{\text{ul},k}^{\text{T}} \tilde{\mathbf{E}}_{\text{B}}^{\text{T}} \tilde{\mathbf{E}}_{\text{B}}^* \hat{\mathbf{h}}_{\text{ul},k}^* \right|^2 \right], \end{aligned} \quad (19)$$

where the cross terms in $\mathbb{E} \left[|\tilde{\mathbf{h}}_{\text{dl},k}^{\text{T}} \hat{\mathbf{h}}_{\text{dl},k}^*|^2 \right]$ vanish because of the orthogonality of the MMSE estimate and the zero-mean property of $\tilde{\mathbf{E}}_{\text{B}}$. Then, using Result 1, the first term in (19), denoted by $\text{CI}_{k,1}$, evaluates to

$$\text{CI}_{k,1} = |\hat{e}_{\text{U},k}|^2 \sigma_{\text{U},k}^2 \left(\left| \text{Tr} \left\{ \Sigma_{\hat{\mathbf{h}}_{\text{ul},k}} |\hat{\mathbf{E}}_{\text{B}}|^2 \right\} \right|^2 + \text{Tr} \left\{ \left(\Sigma_{\hat{\mathbf{h}}_{\text{ul},k}} |\hat{\mathbf{E}}_{\text{B}}|^2 \right)^2 \right\} \right).$$

Next, the second term, denoted by $\text{CI}_{k,2}$ in (19), follows

$$\begin{aligned} \text{CI}_{k,2} &= p_{\text{U},k} \sigma_{\text{B}}^2 \left[\text{Tr} \left\{ \hat{\mathbf{E}}_{\text{B}}^* \Sigma_{\hat{\mathbf{h}}_{\text{ul},k}} \odot \left(\hat{\mathbf{E}}_{\text{B}}^* \Sigma_{\hat{\mathbf{h}}_{\text{ul},k}} \right)^{\text{H}} \right\} \right. \\ &\quad \left. + \text{Tr} \left\{ \Sigma_{\hat{\mathbf{h}}_{\text{ul},k}} \odot \left(\hat{\mathbf{E}}_{\text{B}}^* \Sigma_{\hat{\mathbf{h}}_{\text{ul},k}} \hat{\mathbf{E}}_{\text{B}}^{\text{T}} \right)^{\text{T}} \right\} \right], \end{aligned} \quad (20)$$

where we define $p_{\text{U},k} \triangleq |\hat{e}_{\text{U},k}|^2 (|\hat{e}_{\text{U},k}|^2 + \sigma_{\text{U},k}^2)$. In last step we use Result 2. Then, we evaluate the third term, denoted by $\text{CI}_{k,3}$ in (19), as

$$\text{CI}_{k,3} = p_{\text{U},k} \text{Tr} \left\{ \Sigma_{\hat{\mathbf{h}}_{\text{ul},k}} |\hat{\mathbf{E}}_{\text{B}}|^2 \Sigma_{\hat{\mathbf{h}}_{\text{ul},k}} |\hat{\mathbf{E}}_{\text{B}}|^2 \right\}. \quad (21)$$

The fourth term, denoted by $\text{CI}_{k,4}$, in (19), is computed as

$$\text{CI}_{k,4} = p_{\text{U},k} \sigma_{\text{B}}^2 \text{Tr} \left\{ \Sigma_{\hat{\mathbf{h}}_{\text{ul},k}} \odot \left(\hat{\mathbf{E}}_{\text{B}}^* \Sigma_{\hat{\mathbf{h}}_{\text{ul},k}} \hat{\mathbf{E}}_{\text{B}}^{\text{T}} \right)^{\text{T}} \right\}. \quad (22)$$

Combining $\{\text{CI}_{k,i}\}_{i=1}^4$, we obtain the final expression for the interference due to calibration error at the k -th UE as $\text{CI}_k = \rho \kappa_k \sum_{i=1}^4 \text{CI}_{k,i}$. This is in part constitutes ξ_{kk} in (15e). Finally, we evaluate the multi-UE interference. We first write

$$\mathbf{h}_{\text{dl},k}^{\text{T}} \hat{\mathbf{h}}_{\text{dl},n}^* = \hat{e}_{\text{U},k} \hat{e}_{\text{U},n}^* \hat{\mathbf{h}}_{\text{ul},k}^{\text{T}} \hat{\mathbf{E}}_{\text{B}} \hat{\mathbf{E}}_{\text{B}}^* \hat{\mathbf{h}}_{\text{ul},n}^* + \hat{e}_{\text{U},n}^* \tilde{\mathbf{h}}_{\text{dl},k}^{\text{T}} \tilde{\mathbf{E}}_{\text{B}} \hat{\mathbf{h}}_{\text{ul},n}^*.$$

Then, we can show that

$$\mathbb{E} \left[\left| \hat{\mathbf{h}}_{\text{ul},k}^{\text{T}} \hat{\mathbf{E}}_{\text{B}} \hat{\mathbf{E}}_{\text{B}}^* \hat{\mathbf{h}}_{\text{ul},n} \right|^2 \right] = \text{Tr} \left\{ \Sigma_{\hat{\mathbf{h}}_{\text{ul},k}} |\hat{\mathbf{E}}_{\text{B}}|^2 \Sigma_{\hat{\mathbf{h}}_{\text{ul},n}} |\hat{\mathbf{E}}_{\text{B}}|^2 \right\}.$$

For the power of the second term, we again substitute $\tilde{\mathbf{h}}_{\text{dl},k}$ from (7b). This can be computed similarly to the terms involved in CI_k , thus omitted for brevity. Combining these terms with some algebra, we obtain the SINR as given in Theorem 2. ■

B. Useful Results

Result 1. For a random vector $\mathbf{a} \sim \mathcal{CN}(\mathbf{0}_N, \mathbf{K})$ and a matrix \mathbf{Z} of compatible dimensions, $\mathbb{E}[\mathbf{a}^{\text{H}} \mathbf{Z} \mathbf{a}] = \text{Tr} \{ \mathbf{K} \mathbf{Z} \}$ and $\mathbb{E}[|\mathbf{a}^{\text{H}} \mathbf{Z} \mathbf{a}|^2] = |\text{Tr} \{ \mathbf{K} \mathbf{Z} \}|^2 + \text{Tr} \{ \mathbf{K} \mathbf{Z} \mathbf{K} \mathbf{Z}^{\text{H}} \}$.

Result 2. For a diagonal matrix \mathbf{C} whose diagonal elements are independent and identically distributed (i.i.d.) random variables with zero mean and variance σ_{C}^2 ; and for any two deterministic matrices \mathbf{Z}_1 and \mathbf{Z}_2 of compatible dimensions, it follows that $\mathbb{E}[|\text{Tr} \{ \mathbf{C} \mathbf{Z}_1 \}|^2] = \sigma_{\text{C}}^2 \text{Tr} \{ \mathbf{Z}_1 \odot \mathbf{Z}_1^{\text{H}} \}$ and $\mathbb{E}[\text{Tr} \{ \mathbf{C}^{\text{H}} \mathbf{Z}_1 \mathbf{C} \mathbf{Z}_2 \}] = \sigma_{\text{C}}^2 \text{Tr} \{ \mathbf{Z}_1 \odot \mathbf{Z}_2^{\text{T}} \}$.

These results can be obtained using Isserlis' theorem [16].

REFERENCES

- [1] S. Willhammar *et al.*, "Achieving distributed MIMO performance with repeater-assisted cellular massive MIMO," *IEEE Commun. Mag.*, vol. 63, no. 3, pp. 114–119, Mar. 2025.
- [2] C.-K. Wen *et al.*, "Shaping a smarter electromagnetic landscape: IAB, NCR, and RIS in 5G standard and future 6G," *IEEE Commun. Stand. Mag.*, vol. 8, no. 1, pp. 72–78, Mar. 2024.
- [3] K. Dong *et al.*, "Network-controlled repeater aided time-sensitive communications in urban vehicular networks," *IEEE Wireless Commun. Lett.*, vol. 14, no. 5, pp. 1511–1515, May 2025.
- [4] O. A. Topal *et al.*, "Fair and energy-efficient activation control mechanisms for repeater-assisted massive MIMO," in *23rd Int. Symp. Model. Optim. Mobile, Ad Hoc, Wireless Netw. (WiOpt)*, 2025, pp. 1–7.
- [5] J. Bai *et al.*, "Repeater swarm-assisted cellular systems: Interaction stability and performance analysis," *IEEE Trans. Wireless Commun.*, vol. 25, pp. 10 018–10 034, 2026.
- [6] K. Ueda, K. Arai, and K. Ishibashi, "Performance of repeater-assisted massive MIMO systems: TDD vs FDD," in *Proc. IEEE Int. Conf. Acoust., Speech Signal Process. (ICASSP)*, 2026, pp. 22 307–22 311.
- [7] 3GPP, "New WID on NR network-controlled repeaters," 3rd Generation Partnership Project (3GPP), RP 222673, Sep. 2022, TSG RAN meeting no. 97-e. [Online]. Available: https://www.3gpp.org/ftp/tsg_ran/TSG_RAN/TSGR_97e/Docs/RP-222673.zip
- [8] E. G. Larsson *et al.*, "Reciprocity calibration of dual-antenna repeaters," *IEEE Wireless Commun. Lett.*, vol. 13, no. 6, pp. 1606–1610, Jun. 2024.
- [9] X. Luo, "Multiuser massive MIMO performance with calibration errors," *IEEE Trans. Wireless Commun.*, vol. 15, no. 7, pp. 4521–4534, Jul. 2016.
- [10] A. Minasian *et al.*, "Distributed massive MIMO systems with non-reciprocal channels: Impacts and robust beamforming," *IEEE Trans. Commun.*, vol. 66, no. 11, pp. 5261–5277, Nov. 2018.
- [11] O. Raeesi *et al.*, "Performance analysis of multi-user massive MIMO downlink under channel non-reciprocity and imperfect CSI," *IEEE Trans. Commun.*, vol. 66, no. 6, pp. 2456–2471, Jun. 2018.
- [12] R. Chopra *et al.*, "Blind channel estimation for downlink massive MIMO systems with imperfect channel reciprocity," *IEEE Trans. Signal Process.*, vol. 68, pp. 3132–3145, 2020.
- [13] Y. Ma *et al.*, "Channel estimation error and beamforming performance in repeater-enhanced massive MIMO systems," in *Proc. IEEE 26th Annu. Int. Symp. Pers., Indoor, Mobile Radio Commun. (PIMRC)*, Aug. 2015, pp. 672–677.
- [14] J. Vieira *et al.*, "Reciprocity calibration for massive MIMO: Proposal, modeling, and validation," *IEEE Trans. Wireless Commun.*, vol. 16, no. 5, pp. 3042–3056, May 2017.
- [15] T. L. Marzetta, E. G. Larsson, H. Yang, and H. Q. Ngo, *Fundamentals of Massive MIMO*. Cambridge University Press, 2016.
- [16] L. Isserlis, "On a formula for the product-moment coefficient of any order of a normal frequency distribution in any number of variables," *Biometrika*, vol. 12, no. 1-2, pp. 134–139, 1918.